

LETTERS

Carbon dioxide release from the North Pacific abyss during the last deglaciation

Eric D. Galbraith^{1†}, Samuel L. Jaccard^{1,4}, Thomas F. Pedersen², Daniel M. Sigman³, Gerald H. Haug⁴, Mea Cook⁵, John R. Southon⁶ & Roger Francois¹

Atmospheric carbon dioxide concentrations were significantly lower during glacial periods than during intervening interglacial periods, but the mechanisms responsible for this difference remain uncertain. Many recent explanations call on greater carbon storage in a poorly ventilated deep ocean during glacial periods^{1–5}, but direct evidence regarding the ventilation and respired carbon content of the glacial deep ocean is sparse and often equivocal⁶. Here we present sedimentary geochemical records from sites spanning the deep subarctic Pacific that—together with previously published results⁷—show that a poorly ventilated water mass containing a high concentration of respired carbon dioxide occupied the North Pacific abyss during the Last Glacial Maximum. Despite an inferred increase in deep Southern Ocean ventilation during the first step of the deglaciation (18,000–15,000 years ago)^{4,8}, we find no evidence for improved ventilation in the abyssal subarctic Pacific until a rapid transition ~14,600 years ago: this change was accompanied by an acceleration of export production from the surface waters above but only a small increase in atmospheric carbon dioxide concentration⁸. We speculate that these changes were mechanistically linked to a roughly coeval increase in deep water formation in the North Atlantic^{9–11}, which flushed respired carbon dioxide from northern abyssal waters, but also increased the supply of nutrients to the upper ocean, leading to greater carbon dioxide sequestration at mid-depths and stalling the rise of atmospheric carbon dioxide concentrations. Our findings are qualitatively consistent with hypotheses invoking a deglacial flushing of respired carbon dioxide from an isolated, deep ocean reservoir^{1–5,12}, but suggest that the reservoir may have been released in stages, as vigorous deep water ventilation switched between North Atlantic and Southern Ocean source regions.

The rate at which a portion of the ocean interior exchanges gases with the atmosphere ('ventilation') is reflected by the concentrations of dissolved ¹⁴C and O₂. Both are replenished by exchange with the atmosphere, but whereas ¹⁴C decays at a globally uniform rate, O₂ consumption occurs only where organic matter is respired (Fig. 1). Thus, taken together, these tracers provide complementary information on ocean ventilation and accumulated organic matter respiration, giving key insights into ocean circulation, CO₂ sequestration and nutrient distribution.

The measurement of past variations in the ¹⁴C content of subsurface water masses has long been sought, but has often proven difficult, particularly in waters of the deep Pacific. In theory, the surface-to-deep gradient of Δ¹⁴C (see Fig. 1 legend) can be reconstructed simply by comparing the ¹⁴C/¹²C ratio measured in the carbonate tests of planktonic foraminifera with that of coeval benthic

foraminifera. This approach has provided evidence for reduced ventilation in deep waters of both the Atlantic⁹ and Southern¹³ Oceans, and has shown variable patterns in the upper ocean^{4,14}. However, the broad range among analogous measurements in the deep equatorial Pacific has prompted the suggestion that the ¹⁴C activity of the deep North Pacific during the Last Glacial Maximum (LGM) was no different from that of today^{6,15}. We tested this hypothesis by picking foraminifera in a core raised from 3.6 km water depth in the Gulf of Alaska (Supplementary Information).

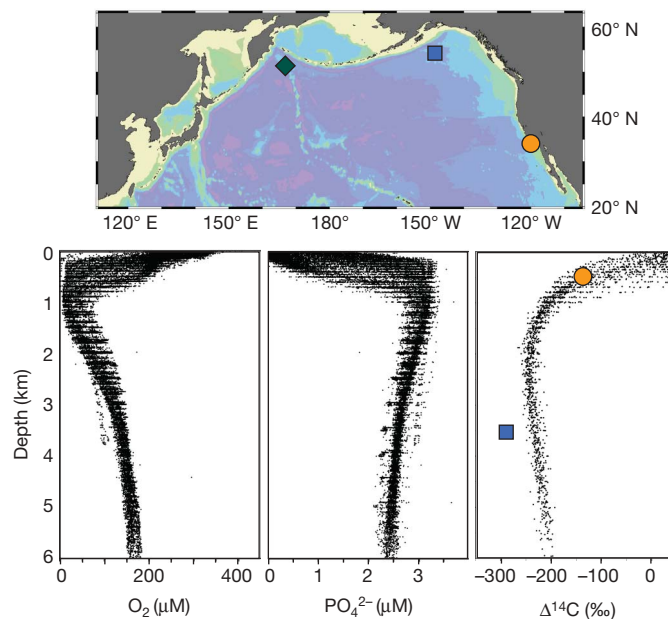


Figure 1 | Dissolved oxygen, phosphate and radiocarbon in the present-day North Pacific. Bottom panel, all measurements available in GLODAP¹⁶ north of 20° N in the Pacific Ocean are shown (see Supplementary Information for additional discussion). Δ¹⁴C is the ¹⁴C/¹²C of DIC expressed as the deviation from the ¹⁴C/¹²C of a standard (see Methods) in ‰. Top panel, locations of core sites GGC-37 (50.42° N, 167.72° E, 3,300 m) and ODP 882 (50.35° N, 167.58° E, 3,244 m) are shown by the dark green diamond, ODP 887 (54.37° N, 148.45° W, 3,647 m) by the dark blue square and ODP 893 by the dark yellow circle. The reconstructed Δ¹⁴C_{cont-atm} (Supplementary Information) of bottom waters at Sites 887 and 893 during the LGM are shown in the bottom right panel as the dark blue square and dark yellow circle, respectively, at their approximate palaeo-depths (120 m less than today).

¹Department of Earth and Ocean Sciences, University of British Columbia, Vancouver, British Columbia V6T 1Z4, Canada. ²School of Earth and Ocean Sciences, University of Victoria, Victoria, British Columbia V8W 3P6, Canada. ³Department of Geosciences, Princeton University, Princeton, New Jersey 08544, USA. ⁴Geological Institute, Department of Earth Sciences, ETH Zürich, Zürich CH-8092, Switzerland. ⁵Department of Ocean Sciences, University of California, Santa Cruz, California 95064, USA. ⁶Department of Earth System Science, University of California, Irvine, California 92697, USA. †Present address: Department of Atmospheric and Oceanic Sciences, Princeton University, Princeton, New Jersey 08544, USA.

Our results, plotted in Fig. 2, show an apparent age difference between co-occurring planktonic and benthic foraminifera during the LGM (18–20 kyr ago) of 1,600–1,900 uncorrected ^{14}C years; this is clearly greater than the apparent age difference of $\sim 1,250$ ^{14}C years near Site 887 today¹⁶. The present results indicate a greater LGM bottom water age than the low-latitude Pacific measurements from 2–2.8 km depth⁶, but are indistinguishable from the planktonic–benthic difference estimated on a core from 3.2 km water depth in the eastern equatorial Pacific (Supplementary Information)¹⁷. Comparison to recently developed reconstructions of atmospheric ^{14}C (Supplementary Information) implies that the ^{14}C activity of the North Pacific at 3.6 km depth, relative to the contemporary atmosphere ($\Delta^{14}\text{C}'_{\text{cont-atm}}$, see Methods), was equivalent to about -290% , a decrease of $\sim 60\%$ from the modern value. This indicates that the deep LGM North Pacific was substantially more isolated than the coeval deep Atlantic Ocean, which was, itself, relatively poorly ventilated ($\Delta^{14}\text{C}'_{\text{cont-atm}} > -215\%$, ref. 12). We note that benthic foraminifera measured at 2.7 km water depth on the New Zealand margin¹³ imply a value of $\Delta^{14}\text{C}'_{\text{cont-atm}}$ of $< -350\%$, consistent with suggestions that deep Southern Ocean waters were more poorly ventilated still⁴.

In contrast to the lower deep ocean, the ventilation of the upper North Pacific during the LGM seems to have been similar to or better than that of today, as previously shown by ^{14}C measurements on the California margin¹⁴ (Figs 1, 2). This observation is consistent with a relatively vigorously circulating, vertically expanded equivalent of the North Pacific Intermediate Water within the upper 2 km of the water column^{7,14}. Together with our results, this shows that the LGM vertical $\Delta^{14}\text{C}$ gradient between intermediate and abyssal waters of the North Pacific was stronger ($>100\%$) than that of today ($\sim 60\%$), supporting the hypothesis that the isolation of LGM abyssal waters involved reduced vertical exchange with the intermediate waters above^{2,5}. We note that this comparison is made only over the short time window of the LGM, as we do not have evidence to test whether this was a persistent feature throughout the glacial period.

Geochemical measurements of LGM sediments from two deep water locations in the subarctic Pacific (Fig. 1) complement our radiocarbon data in characterizing the isolated deep glacial water mass, showing that it bore lower oxygen concentrations and therefore

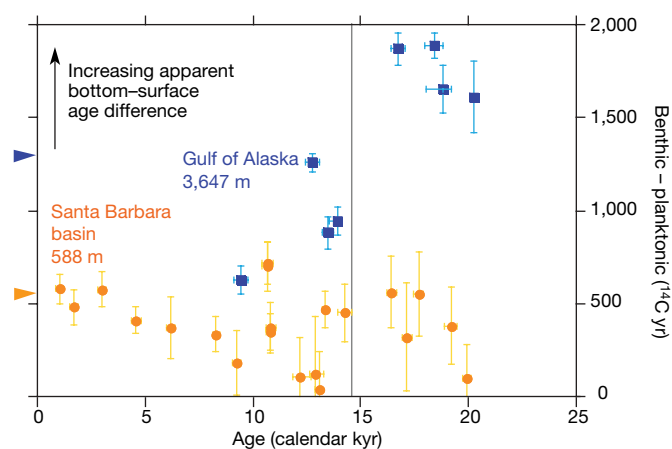


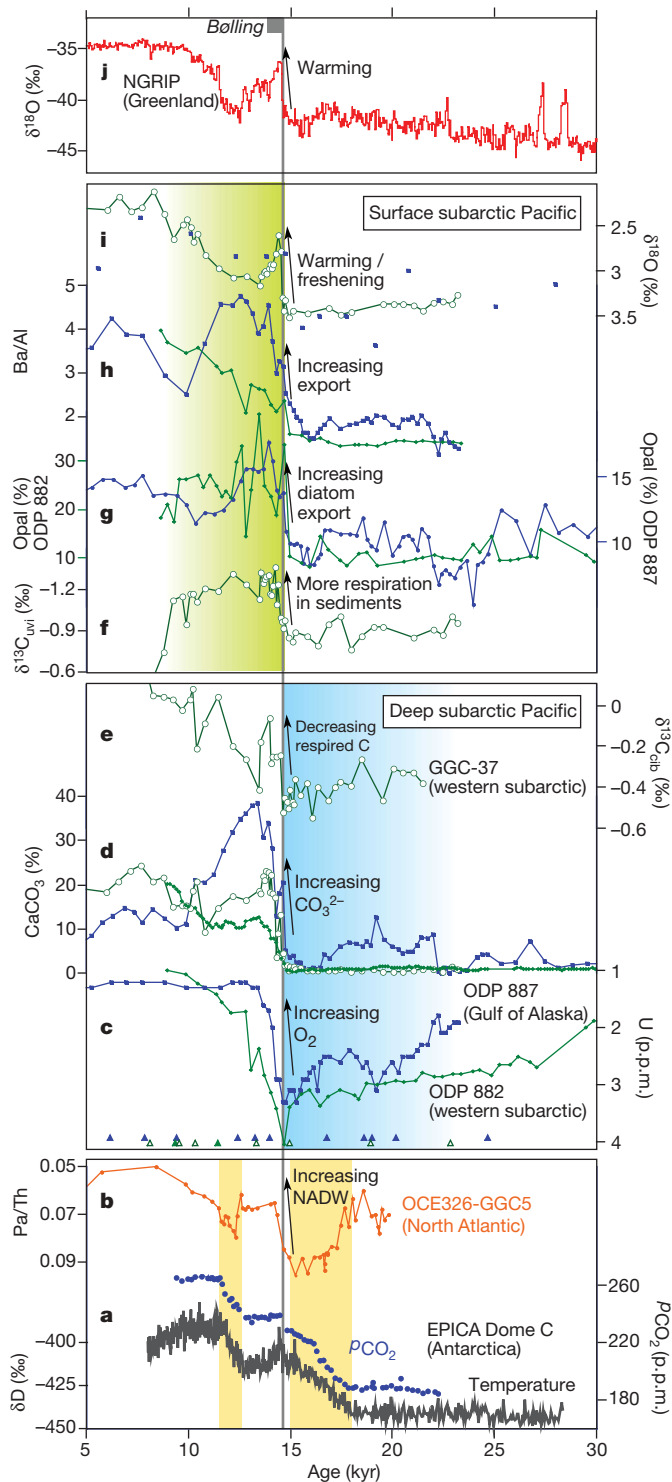
Figure 2 | Apparent age differences between paired benthic and planktonic foraminifera at intermediate and deep sites in the North Pacific over the past 25 kyr. Published data from the upper ocean are shown by dark yellow circles, using the published age model¹⁴. New data from ODP Site 887 are shown as dark blue squares. Differences are calculated from the raw, measured ^{14}C ages. Estimated pre-industrial values for both sites are indicated by the triangles at the left-hand side. The calendar ages used here are the calibrated planktonic ages. Errors are $\pm 1\sigma$ and include errors in the ^{14}C measurement, calendar age calculation and reservoir age. The vertical grey line is drawn at 14.6 kyr ago, as in Fig. 3.

harboured higher concentrations of respired CO_2 . Sediments deposited during the LGM at both locations are enriched in authigenic U (Fig. 3c), which is known to precipitate in oxygen-depleted sediments. Similar glacial U accumulation has been observed at many sites in the deep sea^{1,18,19}, but its interpretation has often been confounded by the possibility that higher organic fluxes caused reducing conditions within the sediments themselves during the LGM, which could theoretically have overwhelmed any effect of bottom water oxygenation. Here, the export production proxies Ba/Al and opal, measured in the same sediments (Fig. 3g, h), show generally reduced fluxes during the last ice age (Supplementary Information), so that the enhanced U accumulation must have resulted from substantially lower bottom water O_2 (ref. 1). This requires the LGM North Pacific at 3–3.6 km depth to have contained a higher concentration of respired carbon than it does today. Although the absence of Mo enrichment (not shown) argues that anoxia did not develop in the vicinity of our core sites, oxygen concentrations may have dropped far below their current concentrations of $\sim 130 \mu\text{M}$ during the LGM.

It is widely thought that the state of the glacial deep ocean was fundamentally determined by Southern Ocean processes^{1–5}, so that the poor ventilation of the deep LGM Pacific would have been related to sea surface conditions near Antarctica. Ice core records show that deglacial warming of the Southern Ocean and a large rise in CO_2 partial pressure (p_{CO_2}) occurred between 18 and 15 kyr ago⁸. During this same period, ^{13}C (ref. 20) and ^{14}C (ref. 4) in the eastern equatorial Pacific thermocline both became progressively depleted, while the atmospheric ^{14}C activity dropped precipitously¹⁵, suggesting that the p_{CO_2} increase was related to the exposure of poorly ventilated deep waters at the surface. Given this evidence, one might expect gradual signs of increased ventilation in the abyssal North Pacific to have accompanied the early southern warming, starting at 18 kyr ago. Surprisingly, the geochemical characteristics of the abyssal subarctic Pacific sediments register no hint of improved ventilation until an abrupt transition about 3 kyr later, witnessed by a host of proxies in the three cores (Fig. 3).

Calcium carbonate (CaCO_3), which was nearly or completely absent in these cores throughout much of the glacial sediment, suddenly appears in abundance at ~ 14.6 kyr ago at each of the three deep subarctic Pacific sites (Fig. 3d, Supplementary Fig. 3). Although increases in local CaCO_3 export may have strongly affected sedimentary CaCO_3 concentrations, the magnitude of change suggests substantially reduced dissolution at the sea floor, implying higher bottom water CO_3^{2-} concentration owing to decreased dissolved inorganic carbon (DIC) and/or increased alkalinity²¹. This implication mirrors high deglacial CO_3^{2-} concentrations previously inferred from foraminiferal Zn/Ca measurements in the deep equatorial Pacific²². An abrupt $>0.3\%$ increase of $\delta^{13}\text{C}$ in the epibenthic foraminifer *Cibicides* over the same sediment interval (Fig. 3e)⁷ is consistent with a rapid reduction of the respired DIC concentration (Supplementary Information), suggesting that this was an important contributor to accelerated CaCO_3 burial.

Over the same sedimentary interval, the $\delta^{18}\text{O}$ of planktonic foraminifera reveals an abrupt freshening and/or warming of surface waters (Fig. 3i)⁷. Within the error of our ^{14}C -based age models (that is, a few centuries, see Supplementary Information) this change in sea surface conditions occurred during the sudden warming in the North Atlantic at the start of the Bølling period (Fig. 3j). Although centennial-scale phasing between the two basins cannot be resolved, the near-synchrony suggests a strong dynamical link. Furthermore, records of ^{14}C within the North Atlantic interior that span the deglaciation^{9,10} describe a pattern of changing ventilation that is remarkably similar to that described here. Like our reconstruction from the North Pacific, Atlantic records show a strengthened vertical ^{14}C gradient during the LGM, with relatively well-ventilated waters overlying extremely ^{14}C -depleted abyssal waters, a situation that clearly persisted in the Atlantic throughout the early CO_2 rise from 18 to 15 kyr ago. This was followed, ~ 14.6 kyr ago, by a rapid ventilation of



deep waters in both basins, when vigorous formation of North Atlantic Deep Water (NADW) resumed^{9–11}. The apparent inter-basin synchrony and chemical homogeneity of the modern abyssal Pacific both suggest that this mid-deglacial ventilation typified a large fraction of the global abyss; the North Pacific and North Atlantic, combined, account for more than 36% of the global ocean volume.

However, although the mid-deglacial ventilation of northern deep waters is synchronous, within chronological uncertainty, with an abrupt ~10 p.p.m. increase of $p\text{CO}_2$ recorded in Antarctic ice⁸ (Fig. 3a), this represents only a small fraction of the total deglacial increase of $p\text{CO}_2$, the majority of which occurred during two phases of Antarctic warming (Fig. 3a). It is perhaps counterintuitive that increased ventilation of such a large deep ocean volume would fail

Figure 3 | Multi-proxy sedimentary records from the subarctic Pacific spanning 5 to 30 kyr ago. New measurements are shown from sites ODP 887 (dark blue squares) and ODP 882 (small dark green diamonds), with previously published data from GGC-37 (open green circles, ref. 7; see Fig. 1 for locations). Proxies reflect the chemical characteristics of bottom waters (c–e), surface water fertility (f–h) and surface temperature/salinity (i). Small triangles show calibrated planktonic ^{14}C dates for ODP 887 (dark blue, filled), ODP 882 (dark green, filled) and GGC-37 (dark green, open). Also shown are published records of Greenland temperature (j, $\delta^{18}\text{O}$, ref. 33), NADW formation (b, Pa/Th, ref. 11) and Antarctic temperature (δD) and CO_2 (a, ref. 8, using the timescale of ref. 4). Note that foraminiferal $\delta^{13}\text{C}$ and $\delta^{18}\text{O}$ records from GGC-37 include additional measurements that were not presented in the original publication (L. Keigwin, personal communication). $\delta^{13}\text{C} = [(^{13}\text{C}/^{12}\text{C})_{\text{sample}} / (^{13}\text{C}/^{12}\text{C})_{\text{standard}} - 1] \times 1,000\text{‰}$; $\delta^{18}\text{O} = [(^{18}\text{O}/^{16}\text{O})_{\text{sample}} / (^{18}\text{O}/^{16}\text{O})_{\text{standard}} - 1] \times 1,000\text{‰}$; the reported values correspond to the Pee Dee Belemnite standard. The blue and green shaded areas highlight the periods before and after 14.6 kyr ago, respectively. The yellow shaded areas indicate the deglacial periods of Antarctic warming, when $p\text{CO}_2$ was increasing.

to cause a more sustained rise in atmospheric CO_2 about 14.6 kyr ago. However, sinking NADW bears low concentrations of unused nutrients, and thus its reinvigoration should have been associated with enhanced net global storage of respired carbon in the ocean interior^{23–25}. We suggest that this occurred through an increase of respired DIC concentrations at intermediate depths, compensating the observed ventilation of deep northern oceans.

Our export production proxy data (Fig. 3) suggest that at least part of this compensatory intermediate-depth carbon storage took place in the North Pacific. Across the same narrow sedimentary intervals that witnessed rapid improvement of deep ocean ventilation, Ba/Al ratios and opal concentrations rise sharply on both sides of the subarctic Pacific (Fig. 3g, h). Although a decrease in the flux of lithogenic material also occurred at this time, ^{230}Th -normalized flux measurements (Supplementary Information) confirm an acceleration in the rain of organic detritus²¹ and siliceous plankton to the sea floor. Further support for a deglacial increase of export production comes from $\delta^{13}\text{C}$ measurements of the infaunal foraminifera *Uvigerina* (Fig. 3f, Supplementary Information)⁷ and from parallel observations throughout the subarctic^{26,27} and northeast Pacific^{28,29}, indicating a basin-wide increase in the rate at which nutrients were supplied to the surface ocean. The apparent coincidence of increased export production in the North Pacific with NADW rejuvenation is also consistent with recent findings from a global ocean-ecosystem model³⁰, whereby greater Atlantic overturning increases the upward flux of remineralized nutrients from the abyss to the global surface ocean. In short, when NADW formation is enhanced, the global thermocline shoals, facilitating the upwelling and entrainment of nutrient-bearing deep waters into the wind-driven circulation.

We therefore suggest that the entrainment of North Pacific deep waters into the wind-driven circulation increased dramatically near the start of the Bølling, accompanied by an enhanced influx of deep waters from the south, establishing a more ‘estuarine’ circulation in the North Pacific. The upward flux of nutrients supported the widespread boom in export production during the Bølling^{26–29}, and the resulting rain of organic matter drove a depletion of oxygen within the upper ocean, explaining the coeval intensification of the intermediate-depth oxygen-minimum zone previously described³¹. Meanwhile, the intense oxygen depletion reflects enhanced storage of respired DIC in the thermocline that counteracted the removal of DIC from the abyssal waters below. Although this minimized the short-term effect on CO_2 , we note that the removal of respired DIC from the deep ocean would have caused the CO_3^{2-} activity there to increase¹², deepening the lysocline; such deepening has long been recognized as a potential mechanism to deplete the oceanic alkalinity inventory and, hence, decrease global CO_2 solubility^{12,22}. Thus, the removal of respired DIC from a large fraction of the deep sea would

have caused an additional, long-term increase of p_{CO_2} (ref. 32), helping to propel the climate system into the interglacial period.

METHODS SUMMARY

Benthic and planktonic foraminifera were hand picked from samples that each spanned a vertical interval of <2 cm, extracted at broad benthic foraminifera abundance peaks (Supplementary Information). Calendar-year ages were calculated assuming a constant subarctic Pacific reservoir age of $\Delta R = 550 \pm 250$ yr (Supplementary Information). Biogenic opal concentrations were determined by molybdate-blue spectrophotometry on alkaline extracts. CaCO_3 concentrations were quantified by coulometric CO_2 determinations, assuming no other carbonate-bearing phase was present. Absolute elemental concentrations of homogenized powders were measured by inductively coupled plasma-mass spectrometry (ICP-MS) for ODP 882, following acid digestion, and by inductively coupled plasma-optical emission spectrometry (ICP-OES) and ICP-MS for ODP 887, following fusion and subsequent dissolution in acid. The age models for ODP 887 and GGC-37 are based exclusively on calibrated planktonic ^{14}C measurements over the deglaciation, whereas that of ODP 882 is also tied to that of the neighbouring core GGC-37 at the midpoint of the rapid CaCO_3 rise (Supplementary Information).

Full Methods and any associated references are available in the online version of the paper at www.nature.com/nature.

Received 17 December 2006; accepted 7 September 2007.

1. Francois, R. *et al.* Contribution of Southern Ocean surface-water stratification to low atmospheric CO_2 concentrations during the last glacial period. *Nature* **389**, 929–935 (1997).
2. Toggweiler, J. R. Variation of atmospheric CO_2 by ventilation of the ocean's deepest water. *Paleoceanography* **14**, 571–588 (1999).
3. Stephens, B. B. & Keeling, R. F. The influence of Antarctic sea ice on glacial–interglacial CO_2 variations. *Nature* **404**, 171–174 (2000).
4. Marchitto, T. *et al.* Marine radiocarbon evidence for the mechanism of deglacial atmospheric CO_2 rise. *Science* **316**, 1456–1459 (2007).
5. Sigman, D. M. & Boyle, E. A. Glacial/interglacial variations in atmospheric carbon dioxide. *Nature* **407**, 859–869 (2000).
6. Broecker, W. *et al.* Ventilation of the glacial deep Pacific Ocean. *Science* **306**, 1169–1172 (2004).
7. Keigwin, L. D. Glacial-age hydrography of the far northwest Pacific Ocean. *Paleoceanography* **13**, 323–339 (1998).
8. Monnin, E. *et al.* Atmospheric CO_2 concentrations over the last glacial termination. *Science* **291**, 112–114 (2001).
9. Robinson, L. F. *et al.* Radiocarbon variability in the western North Atlantic during the last deglaciation. *Science* **310**, 1469–1473 (2005).
10. Skinner, L. C. & Shackleton, N. J. Rapid transient changes in northeast Atlantic deep water ventilation age across Termination I. *Paleoceanography* **19**, doi:10.1029/2003PA000983 (2004).
11. McManus, J. F. *et al.* Collapse and rapid resumption of Atlantic meridional circulation linked to deglacial climate changes. *Nature* **428**, 834–837 (2004).
12. Boyle, E. A. Vertical oceanic nutrient fractionation and glacial/interglacial CO_2 cycles. *Nature* **331**, 55–56 (1988).
13. Sikes, E. L., Samson, C. R., Guilderson, T. P. & Howard, W. R. Old radiocarbon ages in the southwest Pacific Ocean during the last glacial period and deglaciation. *Nature* **405**, 555–559 (2000).
14. Kennett, J. P. & Ingram, B. L. A 20,000-year record of ocean circulation and climate change from the Santa Barbara basin. *Nature* **377**, 510–514 (1995).
15. Broecker, W. & Barker, S. A 190‰ drop in atmosphere's $\Delta^{14}\text{C}$ during the “Mystery Interval” (17.5 to 14.5 kyr). *Earth Planet. Sci. Lett.* **256**, 90–99 (2007).
16. Key, R. M. *et al.* A global ocean carbon climatology: Results from Global Data Analysis Project (GLODAP). *Glob. Biogeochem. Cycles* **18**, doi:10.1029/2004GB002247 (2004).
17. Shackleton, N. J. *et al.* Radiocarbon age of last glacial Pacific deep water. *Nature* **335**, 708–711 (1988).
18. Dezileau, L., Bareille, G. & Reyss, J.-L. Enrichissement en uranium authigène dans les sédiments glaciaires de l’océan Austral. *CR Geosci.* **334**, 1039–1046 (2002).
19. Sarkar, A., Bhattacharya, S. K. & Sarin, M. M. Geochemical evidence for anoxic water in the Arabian Sea during the last glaciation. *Geochim. Cosmochim. Acta* **51**, 1009–1016 (1993).
20. Spero, H. J. & Lea, D. W. The cause of carbon isotope minimum events on glacial terminations. *Science* **296**, 522–525 (2002).
21. Jaccard, S. L. *et al.* Glacial/interglacial changes in subarctic North Pacific stratification. *Science* **308**, 1003–1006 (2005).
22. Marchitto, T. M., Lynch-Stieglitz, J. & Hemming, S. R. Deep Pacific CaCO_3 compensation and glacial–interglacial atmospheric CO_2 . *Earth Planet. Sci. Lett.* **231**, 317–336 (2005).
23. Sigman, D. M. & Haug, G. H. in *Treatise on Geochemistry* Vol. 6 (eds Holland, D. & Turekian, K. K.) 491–528 (Elsevier, Amsterdam, 2003).
24. Ito, T. & Follows, M. J. Preformed phosphate, soft tissue pump and atmospheric CO_2 . *J. Mar. Res.* **63**, 813–839 (2005).
25. Toggweiler, J. R. *et al.* Representation of the carbon cycle in box models and GCMs — 2. Organic pump. *Glob. Biogeochem. Cycles* **17**, doi:10.1029/2001GB001841 (2003).
26. Crusius, J. *et al.* Influence of northwest Pacific productivity on North Pacific Intermediate Water oxygen concentrations during the Bolling–Allerod interval (14.7–12.9 ka). *Geology* **32**, 633–636 (2004).
27. Brunelle, B. G. *et al.* Evidence from diatom-bound nitrogen isotopes for Subarctic Pacific stratification during the last ice age and a link to North Pacific denitrification changes. *Paleoceanography* **22**, doi:10.1029/2005PA001205 (2007).
28. Ivanochko, T. S. & Pedersen, T. F. Determining the influences of Late Quaternary ventilation and productivity variations on Santa Barbara Basin sedimentary oxygenation: a multi-proxy approach. *Quat. Sci. Rev.* **23**, 467–480 (2004).
29. Ortiz, J. D. *et al.* Enhanced marine productivity off western North America during warm climate intervals of the past 52 k.y. *Geology* **32**, 521–524 (2004).
30. Schmittner, A. Decline of the marine ecosystem caused by a reduction in the Atlantic overturning circulation. *Nature* **434**, 628–633 (2005).
31. Zheng, Y. *et al.* Intensification of the northeast Pacific oxygen minimum zone during the Bolling–Allerod warm period. *Paleoceanography* **15**, 528–536 (2000).
32. Broecker, W. & Peng, T. H. The role of CaCO_3 compensation in the glacial to interglacial atmospheric CO_2 change. *Glob. Biogeochem. Cycles* **1**, 15–29 (1987).
33. Andersen, K. K. *et al.* High-resolution record of Northern Hemisphere climate extending into the last interglacial period. *Nature* **431**, 147–151 (2004).

Supplementary Information is linked to the online version of the paper at www.nature.com/nature.

Acknowledgements We thank A. de Vernal, J. Leduc, P. Dulski, M. Soon and K. Gordon for analytical assistance, and J. Sarmiento, R. Toggweiler, M. Kienast, L. Keigwin and S. Calvert for intellectual and practical support. R. Schlitzer’s program Ocean Data View was used to generate Fig. 1. E.D.G., T.F.P. and R.F. were supported by the Natural Sciences and Engineering Research Council of Canada and the Canadian Foundation for Climate and Atmospheric Sciences, S.L.J. by a Swiss National Foundation post-doctoral fellowship, D.M.S. by US NSF, and by BP and Ford Motor Company through the Princeton Carbon Mitigation Initiative, and G.H.H. by Deutsche Forschungsgemeinschaft.

Author Contributions E.D.G. and S.L.J. contributed equally to this work. T.F.P. and G.H.H. initiated and guided the project. E.D.G. prepared samples and picked foraminifera from ODP Site 887, S.L.J. prepared and analysed samples from site ODP Site 882. R.F. and S.L.J. made the ^{230}Th measurements and J.R.S. made the radiocarbon measurements. M.C. contributed to the ^{14}C analysis. E.D.G., S.L.J. and D.M.S. wrote the paper. All authors discussed the results and commented on the manuscript.

Author Information Reprints and permissions information is available at www.nature.com/reprints. Correspondence and requests for materials should be addressed to E.D.G. (egalbrai@princeton.edu).

METHODS

Radiocarbon measurements. Radiocarbon was measured at the UC Irvine Keck AMS facility using the NIST OX1 radiocarbon standard as a reference. All results obtained for the LGM and deglaciation are reported in Supplementary Table 1 according to the conventions of ref. 34. Size-dependent backgrounds were determined using calcite blanks, and were checked by measurements of small aliquots of the IAEA C2 and FIRI turbidite secondary standards. Uncertainties are based on the scatter in repeated measurements as well as counting statistics, and contributions from normalization to the OX1 standard and from background subtraction are included. Ages of planktonic foraminifera were calibrated to calendar years using CALIB 5.0.2 (refs 35, 36).

For the calculations of LGM ^{14}C activity shown in Fig. 1, the $\Delta^{14}\text{C}$ of a given benthic foram sample at the time of calcification was reconstituted to the calibrated age of the coexisting planktonic foraminifera, given the ^{14}C decay rate, providing the palaeo-bottom water $\Delta^{14}\text{C}$ (relative to the modern atmospheric ^{14}C activity). Changes in atmospheric $\Delta^{14}\text{C}$ through time were provided by the IntCal04 compilation³⁷. Comparisons between benthic and atmospheric $\Delta^{14}\text{C}$ were made by the two methods shown in Supplementary Fig. 2, to assess the importance of large secular changes in atmospheric $\Delta^{14}\text{C}$ on the timescales of deep Pacific ventilation ($>1,500\text{ yr}$)³⁸. The raw arithmetic bottom-atmosphere differences calculated directly from these methods are deceiving, however, in that the values are typically reported in terms of their deviation from the relatively low ^{14}C activity of the modern atmosphere, in parts per thousand. To be directly comparable to modern oceanographic measurements of ^{14}C , such as those shown in Fig. 1, we propose a definition of the ^{14}C activity relative to the contemporary atmospheric ^{14}C activity:

$$\Delta^{14}\text{C}' = (\Delta^{14}\text{C}_{\text{bot}} - \Delta^{14}\text{C}_{\text{atm}}) / (\Delta^{14}\text{C}_{\text{atm}} + 1,000) \times 1,000\text{‰}$$

where $\Delta^{14}\text{C}_{\text{bot}}$ is the reconstituted bottom water $\Delta^{14}\text{C}$, and $\Delta^{14}\text{C}_{\text{atm}}$ is the reference palaeo-atmospheric $\Delta^{14}\text{C}$. The values shown in Fig. 1 for ODP 887 and ODP 893 are the averages of all available measurements from 16.4 to 20.5 kyr ago, calculated both as $\Delta^{14}\text{C}'_{\text{proj-atm}}$ and $\Delta^{14}\text{C}'_{\text{cont-atm}}$ (Supplementary Fig. 2). For Site 887, these calculated averages were $-295 \pm 38\text{‰}$ and $-286 \pm 32\text{‰}$, respectively ($\pm 1\sigma$, $n = 4$), while for Site 893 they were $-153 \pm 36\text{‰}$ and $-137 \pm 35\text{‰}$, respectively ($n = 5$). An estimate of the minimum possible ventilation decrease at Site 887 can be made by assuming a very small LGM reservoir age of $\Delta R = 250\text{ yr}$, which gives $\Delta^{14}\text{C}'_{\text{proj-atm}}$ and $\Delta^{14}\text{C}'_{\text{cont-atm}}$ of $-272 \pm 28\text{‰}$ and $-257 \pm 19\text{‰}$, respectively.

Geochemical measurement methods. All analyses were made on freeze-dried and homogenized samples. Biogenic opal percentage was determined by alkaline extraction of silica³⁹. Replicate measurements indicate a reproducibility of $\pm 3\%$. For ODP 882, absolute elemental concentrations of U, Ba and Al were measured by ICP-MS (ELAN 5000A) using solution nebulization after mixed acid

digestion (HF-HClO_4) under pressure. Precision and accuracy were better than 5%. For ODP 887, samples were fused with LiBO_2 at 1,273 K and the resulting glass dissolved in HNO_3 . Using aliquots of the same solutions, absolute elemental concentrations of Al were measured by ICP-OES (Varian Vista Pro) while U and Ba were measured by ICP-MS (ELAN 9000) by ALS Chemex Ltd. Accuracy was better than 5%, 5% and 2%, respectively, for replicate measurements. All CaCO_3 concentrations were measured by coulometry as described²¹.

Age models. The age model for ODP 887 is based on 12 planktonic ^{14}C ages (Supplementary Table 2), calibrated as described above with $\Delta R = 550 \pm 250\text{ yr}$. Changes in reservoir age are likely to have rendered the median calibrated values inaccurate at most times, but the true values should tend to lie within the error limits, if these are accurately estimated. Therefore, we chose three values at the calibrated 1σ error limits and one at the calibrated 2σ error limit that minimize changes in sedimentation rate (see selected ages, Supplementary Table 2). The age model was linearly interpolated between the selected ages.

For GGC-37, the published ^{14}C ages of ref. 8 were recalibrated using Calib 5.0.2 with a reservoir age ΔR of $550 \pm 250\text{ yr}$. The suggestion that reservoir ages in this region changed markedly between 12.8 and 13.3 ^{14}C kyr BP (ref. 40) calls into question the reliability of ^{14}C ages within this interval. We therefore did not include ^{14}C ages within this interval, in favour of a constant sedimentation rate. This conservative approach suggests that the midpoint of the rapid CaCO_3 concentration rise was at ~ 14.5 kyr ago, compared to the age of 15.3 kyr ago suggested by the age model of ref. 7. The age model for ODP 882 is tied to the age model of the nearby core GGC-37 at the midpoint of the rapid CaCO_3 rise (Supplementary Information), supplemented with two calibrated planktonic radiocarbon ages (at 9.8 and 12.0 kyr ago), and linearly interpolated between age ties to coincide with the age model of ref. 21 at 30 kyr ago. Note that the age model for ODP 887 remains completely independent of the other records, and no attempt was made to improve the fit of the planktonic $\delta^{18}\text{O}$ records to the Greenland temperature record.

34. Stuiver, M. & Polach, H. A. Reporting of ^{14}C data. *Radiocarbon* **19**, 355–363 (1977).
35. Stuiver, M. & Reimer, P. J. Extended ^{14}C data base and revised CALIB 3.0 ^{14}C age calibration program. *Radiocarbon* **35**, 215–230 (1993).
36. Hughen, K. A. *et al.* Cariaco Basin calibration update: Revisions to calendar and ^{14}C chronologies for core PL07–58PC. *Radiocarbon* **46**, 1161–1187 (2004).
37. Reimer, P. J. *et al.* IntCal04 terrestrial radiocarbon age calibration, 0–26 cal kyr BP. *Radiocarbon* **46**, 1029–1058 (2004).
38. Adkins, J. F. & Boyle, E. A. Changing atmospheric $\Delta^{14}\text{C}$ and the record of deep water paleoventilation ages. *Paleoceanography* **12**, 337–344 (1997).
39. Mortlock, R. A. & Froelich, P. N. A simple method for the rapid-determination of biogenic opal in pelagic marine-sediments. *Deep-Sea Res. A* **36**, 1415–1426 (1989).
40. Sarnthein, M. *et al.* Warmings in the far northwestern Pacific promoted pre-Clovis immigration to America during Heinrich event 1. *Geology* **34**, 141–144 (2006).